INDIAN JOURNAL OF SCIENCE AND TECHNOLOGY

RESEARCH ARTICLE

OPEN ACCESS

Received: 21-07-2022

Accepted: 31-10-2022

Published: 09-12-2022

Citation: Singh MK, Anbazhahan N, Gowtham B (2022) An Integrated assessment on LULC changes and Groundwater Quality in Ambattur Zone of Metropolitan Chennai, India. Indian Journal of Science and Technology 15(46): 2515-2526. https://doi.org/10.17485/IJST/v15i46.1519

* **Corresponding author**.

mayanksingh3008@gmail.com

Funding: None

Competing Interests: None

Published By Indian Society for Education and Environment (iSee)

ISSN
Print: 0974-6846
Electronic: 0974-5645

An Integrated assessment on LULC changes and Groundwater Quality in Ambattur Zone of Metropolitan Chennai, India

Mayank Kumar Singh[1]*, N Anbazhahan[2], B Gowtham[3]

1 Ph.D. Scholar, Department of Geography, Presidency College, Chennai, 600005, Tamil Nadu, India
2 Assistant Professor, Department of Geography, Presidency College, Chennai, 600005, Tamil Nadu, India
3 Assistant Professor, Department of Geology, Presidency College, Chennai, 600005, Tamil Nadu, India

Abstract

Objectives: The current study shows the magnitude of changes in land use and land cover (LULC) in the Ambattur Zone from 1990 to 2021 and examines its impact on groundwater quality through the Gibbs diagram, Piper diagram, multivariate statistical analysis, and water quality index (WQI) for drinking. **Methods:** Landsat images were collected to derive the LULC images through the supervised classification approach. Groundwater samples were collected from 31 wells for two seasons and analyzed for the hydrogeochemical study. Gibbs, Piper, multivariate statistical analysis and WQI were done to evaluate the groundwater quality for drinking purpose and to study the hydrogeochemical characteristics. **Findings:** The results show that barren land decreased from 7.4 to 4.31 km^2, whereas, built-up land expanded from 21.37 to 24 km^2. Compared to barren and built-up regions, water and vegetation land haven't changed much. LULC change analysis required assessing Ambattur groundwater quality. Physico-chemical investigations and ionic concentrations show that Ambattur industrial zone groundwater is contaminated and unsafe for human consumption. WQI shows that 60% of groundwater is unfit in both seasons. Evaporation and rock-water interaction alter the area's groundwater chemistry. Hydrogeochemical facies diagrams show alternating alkaline and alkali dominance, as well as strong and weak acids. According to correlation matrices, all analytical parameters except pH have a positive correlation. Four basic components and a cluster contribute to understanding industrial pollution. **Novelty:** (i) The present study integrates LULC changes and hydrogeochemistry for the evaluation of groundwater quality. (ii) The comprehensive approach of analyzing LULC changes in conjunction with evaluating the groundwater geochemistry gives new insights in groundwater management for the long-term development of any region.

Keywords: Landsat; Supervised classification; LULC changes; Hydrogeochemistry; WQI; Multivariate statistics

1 Introduction

The elixir of all life is water, on which human actions have a significant negative impact. Since the industrial revolution, natural and contaminated waters have been extensively investigated throughout the globe. The site-specific development has damaged and continues to pollute the groundwater system in multiple locations across India[1–4]. Due to a lack of surface water resources, economic development in arid and semi-arid areas is increasingly dependent on groundwater, which provides high-quality water for drinking, household, agricultural, and industrial purposes. This puts strain on groundwater aquifers, which causes them to degrade and become unsaturated, which is a problematic condition[5,6]. Over exploitation of groundwater as a result of rapid urbanisations and industrial expansion causes groundwater level depletion. Polluting effluents from urban residents and industries have a negative impact on groundwater quality. This shows the need for LULC (Land Use and Land Cover) change analysis, a key tool, can be used to evaluate the effects of human activity on the environment. A basic inventory of the land's resources is provided via land cover mapping. A thorough examination of land use and land cover change can also reveal the rate of deforestation and the most important routes for changing forested land[7]. According to the 2011 census, Chennai, the capital of Tamilnadu, is the fifth most populous metropolitan area in India[8]. Its periphery is home to a number of industrial areas[9]. Due to the influx of residents, Chennai City has seen its level of urbanisation rapidly develop as well as its population grow in recent years. This has put further strain on the metropolitan city's needs for a living. The ecosystem is so overburdened by increased human demands, further urbanisation, and industrial activities that it is unable to regenerate. Overall, under various environmental, political, demographic, and social circumstances, land use practises increase over an extended period of time. With the aid of GIS technologies and expertise in remote sensing, this has to be monitored and understood[10]. The mapping of the land use and land cover of a region can be done with the help of remote sensing and GIS techniques. The integration of remote sensing data with GIS provides numerous new views and opportunities for the analysis, evaluation, and interpretation of data in conjunction with supplementary digital information, such as digitised maps[11]. Numerous studies have evaluated the hydrogeochemistry of parts of the Chennai region, to identify the groundwater suitability for drinking, domestic, irrigation, and industrial purposes. In those previous studies, the LULC changes were not considered primarily for the groundwater contamination. A comprehensive approach integrating the LULC change analysis with hydrogeochemical studies has not been done so far. Temporal development activities in cities like Chennai play a vital role in freshwater demand and groundwater abstraction. Encroachments by residential and industrial expansions over the surface water resources reduce the natural recharge and increase the need for the freshwater. The industrial activities have released untreated effluents into the recharging zones, which has led to the contamination of groundwater. Although regular monitoring of groundwater quality is of utmost importance in such residential and industrial sectors. It will help in finding out the quality changes that have been taking place over the years. Land use and land cover information about landscape patterns, changes, and interactions between human activities and natural occurrences is essential for effective land management, planning, and decision-making involving the earth's surface[12,13]. The present study was carried out to show the extent of changes in land use and land cover of the Ambattur Zone for the period of 40 years (from 1990 to 2021) and to examine its impact on groundwater quality through the Gibbs diagram, Piper diagram, Multivariate statistical analysis, and Water quality index (WQI) for its use as a drinking purpose. The primary aim of this study is to protect the existing water, free from contaminants and minimise the contaminants by identifying the source and cause of pollutants.

2 Methodology

2.1 Study Area

As shown in Figure 1, the industrial zone of Ambattur is situated between the latitudes of 13°3'0" and 13°9'0"N and longitudes of 80°8'0" and 80°13'0"E. The region's geology is composed of crystalline rocks from the Archean era, cemented Gondwana, tertiary sediments, and modern alluvium deposits. Grey brown to black sandy clay is the chief geological formation that occupies most of the eastern regions of the study area. In the western part, laterite and lateritic gravel are being found as the second dominant rock type. Sandstone formations were found as patches along with the lateritic formation in the western region to north part of the study area. Several different types of small and large-scale enterprises can be found in this neighbourhood. Underground water is the only source of water for Ambattur's industrial zones. The quality of the groundwater in this area is steadily declining as a result of industrial activities. The annual average temperature is between 24.3°C and 32.9°C. The district has 1285.6 to 1232.7mm of yearly rainfall on average. Ambattur is a neighbourhood in western Chennai that is part of the Thiruvallur district of Tamil Nadu's Ambattur Taluk of the Chennai Corporation. The Chennai Corporation classifies the Ambattur Zone, which has 15 wards, as the VII Zone (ward numbers 79 to 93).

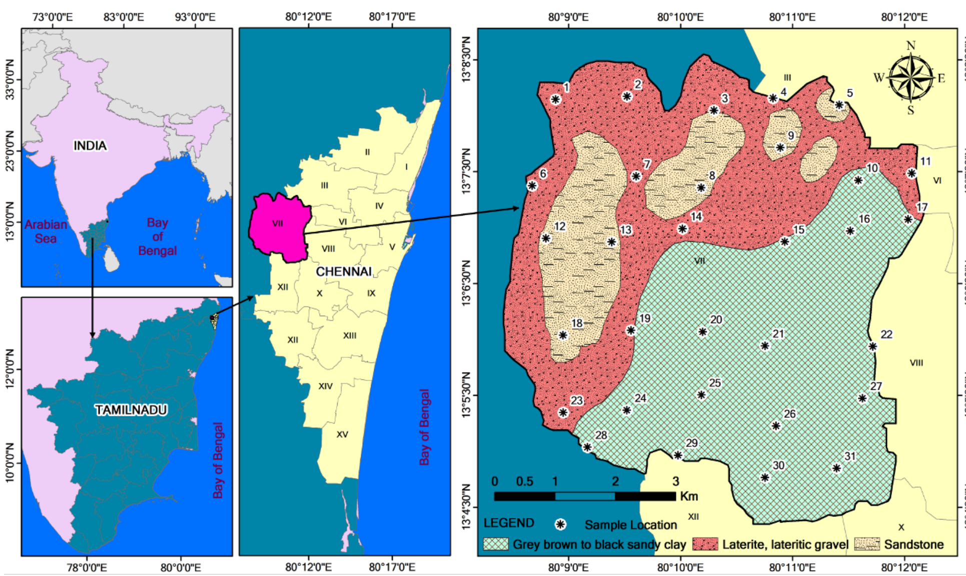

Fig 1. Geology of Ambattur industrial block with sample locations

Geological Survey of India maps scaled at 1:50,000 were used to prepare the base map for the study area (Figure 1). Landsat cloud free images of 30m resolution from the USGS portal for the years 1990, 2000 and 2021 were downloaded and registered in the ArcGIS 10.3 software [imagery particulars are given in the Table 1]. Pre-processed satellite images are loaded into the ERDAS GIS platform[14,15]. True colour composite maps were produced using the red, green, and blue bands (RGB) of each scene in the module "RGB Composite". Subsequently, false colour maps (FCC) using the bands Green, Red, and Infra-red (RGIR) were produced in the same module "RGB Composite" for both scenes[16,17]. These two composite maps are used later in assigning the classes for each cluster of classified images. A supervised classification approach was applied to classify the LULC[18]. Since the study area is small, 100 region of interest (ROI) polygons grouped into four classes were generated through the visual interpretation with the support of RGB and FCC maps. Based on the ROI, supervised classification was performed and 4 classes such as barren, built-up land, vegetations and water bodies were derived (Figure 2). The barren land class represents all the unused lands, waste lands, uncultivated lands, open scrubs, and sandbars. The built-up land denotes the residential areas, industrial constructions, and pavements. The class vegetation covers all agriculture fields, forest, bushes, and scrubs. All the waterlogged areas were grouped into the water body class. Using the geometry calculator tool in the attribute table of the ArcGIS software, the area of each class was found.

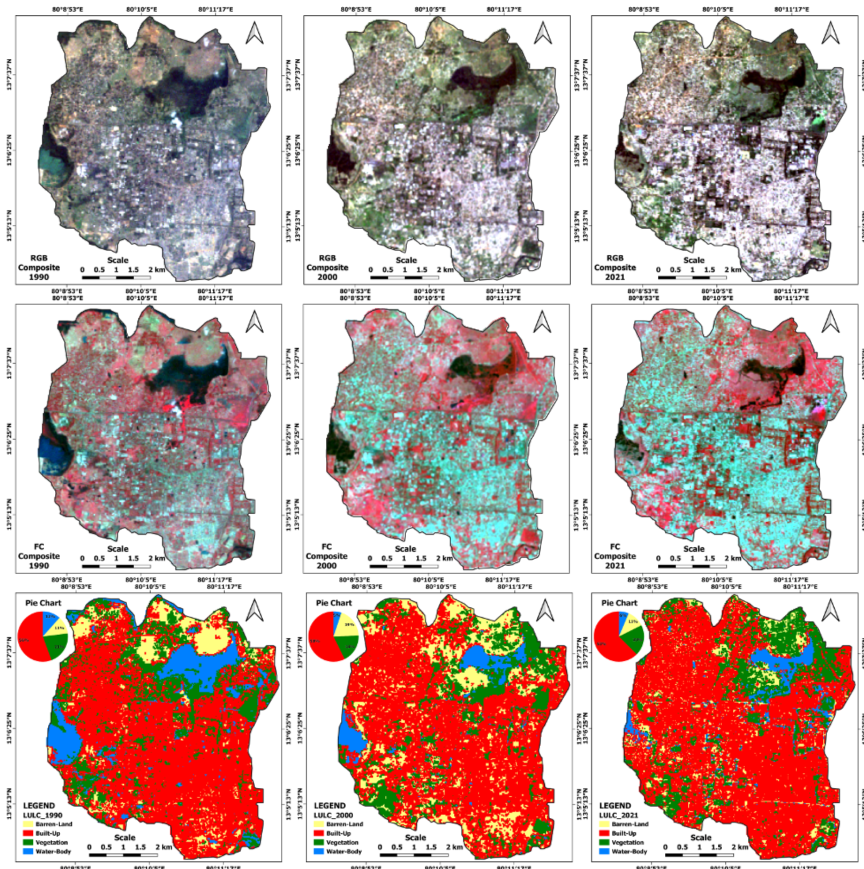

Fig 2. True colour composite(RGB), False colour composite (GRIR) and Land use/Land cover (LULC) maps forthe years 1990, 2000 and 2021

Table 1. Thesatellite imagery particulars and the calculated area of LULC Classes

Scene Year	**1990**	**2000**	**2021**
Landsat Scene Identifier	LT51420511990074ISP00	L71142051_05120001028	LC81420512021111LGN00
Acquisition Date	15-03-1990	28-03-2000	21-04-2021
WRS Path	142	142	142
WRS Row	51	51	51
Sensor Identifier	TM	ETM+	OLI_TIRS
Class	**LULC Class Area in km2 (%)**		
Water-Body	4.46 (11.62)	1.97 (5.13)	2.45 (6.38)
Barren-Land	4.38 (11.41)	7.4 (19.28)	4.31 (11.23)
Vegetation	8.18 (21.31)	7.01 (18.26)	7.63 (19.87)
Built-Up	21.37 (55.67)	22.01 (57.33)	24 (62.52)
Total	38.39 (100)	38.39 (100)	38.39 (100)

Groundwater samples were collected from 31 well sites during June 2020 as a premonsoon and during January 2021 as postmonsoon. As many sites as possible were sampled using a grid pattern sampling technique to provide adequate coverage of the study area. With the use of a handheld Garmin GPS unit, sample geographic coordinate locations are acquired. The American Public Health Association's suggested analysis techniques are used for chemical analysis[19]. Using portable EC and pH metres, in-field measurements of electrical conductivity, total dissolved solids, and pH were made. Na and K were determined using a flame photometer, while Ca and Mg were determined using the EDTA titration method. Acid titration was used to estimate HCO_3, argentometry was used to determine Cl concentration, and a spectrophotometer was used to determine SO_4 and NO_3 using the turbidity method. Titrimetric analysis is used to determine the total hardness and total alkalinity of $CaCO_3$. The descriptive statistics of the levels of the physicochemical parameters are given in Table 2. With the use of AquaChem 5.0 software, the findings were shown as Piper trilinear and Gibbs plots, and SPSS v16 was utilised for multivariate statistical analysis. The water quality index was derived by giving weight (wi) to the physicochemical parameters based on their relative importance in the overall quality of drinking water as shown in Table 2. All the parameters, including calcium, magnesium, sodium, pH, nitrate, etc., were given a weight of 1 to 5 based on their significance in determining water quality[20–22].

Table 2. Results range of chemical parameters and relative their weight

Parameters	Pre-Monsoon		Post-Monsoon		Weight (wi)	Relative Weight (Wi)	WHO Standard
	Range	Mean	Range	Mean			
EC	1067-11450	3158	460-13280	2821.9	-	-	-
pH	7.0-7.9	7.3	6.9-8.6	7.53	5	0.161	6.5
Ca	58-690	178	38-740	195	4	0.129	100
Mg	20-574	103.9	7-644	89.71	3	0.096	50
Na	47-868	295	16-1481	246.6	3	0.096	200
K	0-68	14.1	1-137	19.29	2	0.064	20
HCO3	203-722	389	92-769	346.3	-	-	-
SO4	34-493	178	4-768	178.2	2	0.064	200
Cl	179-3038	675.8	27-4254	645.7	3	0.096	250
NO3	1-140	45	1-169	45.61	3	0.096	45
F	0.25-1.26	0.6	0.26-1.88	0.7	1	0.032	1.5
TDS	584-5582	1706	252-7438	1599	5	0.161	500
CaCO3 (TH)	254-4766	1013.5	145-4100	857.25	-	-	-
CaCO3 (TA)	165-591	324	75-630	292.09	-	-	-
					Σwi=31	ΣWi=1	

The relative weight (Wi) is calculated as per the formula

$$Wi = \frac{wi}{\sum_{i=1}^{n} w\,i} \quad (1)$$

Where n is the number of parameters being assessed by WQI. wi is the weightage assigned to each parameter. Each parameter is assigned a quality rating scale (qi)

$$qi = \frac{Ci}{Si} \times 100 \quad (2)$$

Where 'Ci' is the obtained value of each parameter and 'Si' is the standard values as recommended by WHO[23].

$$\mathrm{SI}_i = W_i \times qi \quad (3)$$

Where SI_i is the sub-index of ith parameter

$$\mathrm{WQI} = \sum \mathrm{SI}_i \quad (4)$$

3 Result and Discussion

The results of the groundwater analytical parameters are compared with the drinking water guideline values proposed by the World Health Organisation. So far, no studies have been conducted exclusively in the Ambattur industrial zone for comparative analysis. Some studies have been done on regional scales, which are unsuitable to compare with the results of the present study, since the present study was conducted in smaller area. Moreover, the hydrogeochemistry of any region in the world is unstable and more dynamic in nature, so periodical monitoring is required to ensure the appropriateness of water quality for various purposes.

3.1 LULC changes

According to the obtained results, the overall area of classes that existed at the time of the image taken is illustrated in the pie charts of the LULC maps. In 1990, the built-up land covered 55.67% of the total area, followed by 21.31% vegetation cover, 11.62% water and 11.41% barren land. During 2000, built-up land covered 57.33% of the total area, followed by barren land of about 19.28%, whereas vegetation covered an area of 18.26% and water bodies occupied 5.13%. In 2021, the area of built-up land was increased by 62.52% and vegetation cover increased by 19.87%. The Waterlogged area was raised to 6.38% and the area of barren land was decreased to 11.23%. Since Chennai is a rapidly developing city, the demand for land to establish constructions is very high. Hence, the barren lands are mostly converted into built-up land. In 4 decades, about 3.09 km^2 of barren land was changed into built-up, vegetation, and water-logged land. Since 1990, nearly 2.63 km^2 of land has been used for new built-ups. The rate of increase of built-up land is 0.066 km^2/year. The temporal change in the total area of vegetation and water bodies depends upon the availability of fresh water in the surface storage systems and monsoonal precipitation. The inferences from the LULC changes show that the expansion of industrial and residential built-ups undoubtedly increases the demand for freshwater supply and pushes towards overexploitation of groundwater. The untreated effluents from the industrial activities and waste water sewage from the residential settlements mix with the surface water systems and reach into the groundwater environment through the recharging process. It adversely affects the groundwater quality and makes it unsuitable for any utilisation. Hence, monitoring the groundwater quality is essential to ensure the availability of freshwater for basic demands of the study area.

3.2 Groundwater Quality

Premonsoon pH levels range from 7.0 to 7.9, and postmonsoon pH values range from 6.9 to 8.6. The current study demonstrates that the groundwater in the study area is within the standard limit in both seasons for the pH range that the WHO has set for drinking water, which is 6.5 to 8.5, except for sample 27 in postmonsoon. Premonsoon electrical conductivity values range from 1067 to 11450 μS/cm, and postmonsoon values range from 460 to 13280 μS/cm. During premonsoon and postmonsoon, the total dissolved solids of the groundwater samples ranged from 584 to 5582 mg/L and 252 to 7438 mg/L, respectively. It has been discovered that 25.8 percent of premonsoon samples and 22.6 percent of postmonsoon samples have TDS levels that are over the recommended limit of 2000 mg/L and are therefore unsafe for human consumption. According to their mean value in both seasons, sodium is the predominant cation, followed by calcium, magnesium, and potassium. According to their mean concentration of anions in both seasons, the order of abundance is chloride, followed by bicarbonate, sulphate, nitrate, carbonate, and fluoride.

During the premonsoon, the values for total hardness and total alkalinity range from 254 to 4766 mg/L and from 165 to 591 mg/L, respectively. The same ranges between 145 mg/L and 4100 mg/L and 75 mg/L to 630 mg/L in the postmonsoon. Comparing the ionic concentrations of groundwater to the recommended drinking water levels reveals that, during premonsoon, 12.5% of samples exceeds the limit of 200 for Ca, 25.8% of samples exceeds the limit of 100 for Mg, 19.4% of samples exceeds the limit of 1000 for Cl, 6.5% of samples exceeds the limit of 400 for SO_4, 48.4% samples exceed the limit of 45 for NO_3 and the 48.4% of samples exceeds the limit of 600 for TH. A comparative investigation reveals that during postmonsoon, 25.8%, 16.1%, 19.4%, 12.9%, 45.2%, 6.5%, and 35.5% of the groundwater samples were, respectively, unfit for consumption due to Ca, Mg, Cl, SO_4, NO_3, F, and TH limits. In the study location, various chemicals indicate varying levels of groundwater suitable for drinking.

Since the quantity of potable water varies according to the concentration limits of various chemicals found in groundwater, WQI was computed to find the overall quantity of potable groundwater in the study area. The WQI findings are categorised as follows: excellent as <50, good as 50 to 100, poor as 100 to 200, very poor as 200 to 300, and unsuitable as >300 for drinking. In the premonsoon season, 54.83% of the groundwater is poor for human consumption, followed by 19.35% of good, 16.12% of very poor, and 9.67% of unsuitable groundwater for drinking (Table 3).. The postmonsoon WQI indicates that 38.7% of groundwater quality poor for drinking, 32.25% is good, 12.9% is unsuitable, 9.6% is very poor, and only 6.45% of groundwater is excellent for drinking. The untreated industrial waste water mixed with surface water and made its way into the groundwater system of the study area. This made the groundwater less clean.

Table 3. Water Quality Index (WQI) for groundwater samples

Range	Category	Pre-Monsoon		Post-Monsoon	
		No. of samples	Values in %	No. of samples	Values in %
<50	Excellent	0	0	2	6.45
50-100	Good	6	19.35	10	32.25
100-200	Poor	17	54.83	12	38.7
200-300	Very Poor	5	16.12	3	9.6
>300	Unsuitable	3	9.67	4	12.9

3.3 Hydrogeochemical Processes

Gibbs postulated that precipitation, rock-water contact, and evaporation are the three fundamental factors governing the chemistry of groundwater[24]. In the present study, the analytical values are plotted on Gibbs' diagram, and it is determined that evaporation and rock-water interaction are the most important determinants of groundwater chemistry in this location. About 58.1% of the cation compounds and 54.8% of the anion compounds in the groundwater were controlled by an evaporation mechanism during the premonsoon season. With regard to cation and anion compounds, rock-water interaction controls 64.5% and the evaporation process controls 51.6% of the groundwater chemistry during the post-monsoon season (Figure 3). Evaporation causes a rise in the ionic content of groundwater in the research area.

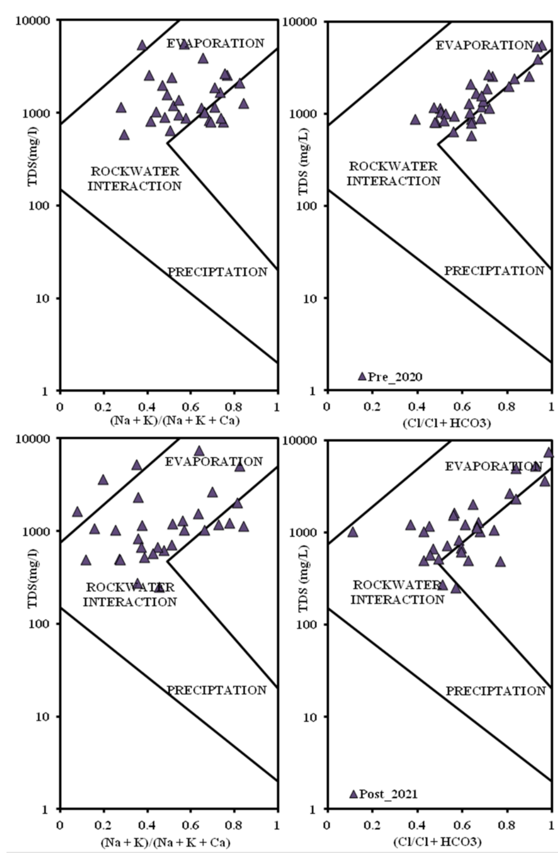

Fig 3. Gibb's plot for pre-monsoonand post-monsoon results

The Piper trilinear diagram illustrates various hydrogeochemical faces based on the relative abundance and chemical equilibrium of the ions found in groundwater[25]. The premonsoon groundwater samples of about 58.1% and the postmonsoon groundwater samples of about 74.2% in the present investigation had Ca+Mg (alkaline earth) exceeding the Na+K (alkali earth) and 96.8% of the samples in both seasons fell into the SO_4+Cl (strong acids) exceeding the CO_3+HCO_3 (weak acids) class. During premonsoon, the subcategories of the diamond-shaped plot reveal that the Na-Cl type is predominant at 41.9%, followed by the Ca-Mg-Cl type at 32.3%, the Ca-Mg-SO_4 type at 22.6%, and the Na-HCO_3-Cl type with 3.2%. It shows that industrial waste and the dissolving of formation salts have a crucial influence on the hydrogeochemistry of the groundwater in the research region. In the postmonsoon season, the predominant type of groundwater is Ca-Mg-Cl (48.4%), followed by Ca-Mg-SO_4 (25.8%), Na-Cl (22.6%), and Na-HCO_3-Cl (3.2%) (Figure 4). The play of precipitating freshwater mixing with groundwater in the study area was shown by the increase in the number of Ca-Mg ionic faces.

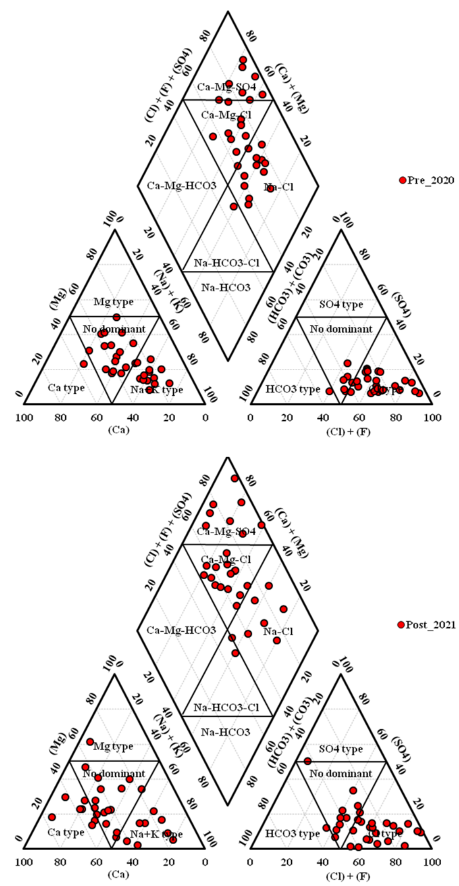

Fig 4. Piper plot for pre-monsoonand post-monsoon results

3.4 Multivariate Analysis

The statistical correlations between 14 hydrogeochemical parameters are studied. The correlation matrix for the analytical results of the groundwater samples collected during both the pre and post-monsoon seasons is shown in Table 4. In premonsoon, strong positive associations (>0.75) were observed between the parameters such as EC with TDS, Ca, Mg, Na, Cl, and SO_4; TDS with Ca, Mg, Na, Cl, and SO_4; Ca with Mg and Cl; Mg with Cl, and TA with HCO_3. Whereas, a moderate correlation (0.5 – 0.75) was discovered between parameters such as EC and TH; TDS and TH; TH with Ca, Mg, and Cl; Ca with Na, SO_4, and F; Mg with Na, SO_4 and F; Na with SO4, Cl and F; SO_4 with Cl and Cl with F. Weak correlations (0.3-0.5) were obtained between the parameters such as TH with F; TA with Na; Na with HCO_3 and SO_4 with F. All of the major anions and cations have a positive correlation, indicating that the research region was primarily affected by silicate weathering and had a significant impact from anthropogenic effluents. In the correlation of post-monsoon results, the EC and TDS demonstrate a substantially positive association with TH, Ca, Mg, Na, Cl, and SO_4. The moderate correlation of K with NO_3 distinctly explains the mixed irrigation return flow that carries the dissolved K-fertilisers. A strong positive correlation between SO_4 and Cl with Ca, Mg, and Na shows the weathering and dissolution of anhydrite and halite.

Table 4. Pearson's correlation matrix for the analytical values

Parameters	EC	TDS	Ph	TH	TA	Ca	Mg	Na	K	HCO_3	SO_4	Cl	NO_3	F
														Post-Monsoon
EC	1	1	-0.04	0.9	0.13	0.83	0.88	0.81	0.05	0.15	0.86	0.99	-0.3	0.17
TDS	0.99	1	-0.03	0.89	0.15	0.82	0.87	0.82	0.07	0.17	0.86	0.99	-0.28	0.15
Ph	-0.17	-0.16	1	-0.15	-0.13	-0.27	-0.04	0.13	-0.07	-0.2	-0.07	-0.01	-0.05	-0.12
TH	0.66	0.66	-0.11	1	-0.11	0.94	0.97	0.48	0.02	-0.09	0.84	0.91	-0.33	0.18
TA	0.01	0	0.06	-0.18	1	0.02	-0.2	0.4	0.21	0.98	0.14	-0.01	0.31	0.21
Ca	0.89	0.91	-0.35	0.71	-0.18	1	0.82	0.4	0.17	0.04	0.81	0.81	-0.24	0.19
Mg	0.95	0.94	-0.24	0.7	-0.2	0.92	1	0.49	-0.1	-0.18	0.79	0.91	-0.36	0.17
Na	0.83	0.81	0.03	0.4	0.36	0.54	0.66	1	0.04	0.42	0.63	0.77	-0.19	0.07
K	0.15	0.14	0	0.02	0.28	0.1	-0.01	0.19	1	0.23	-0.2	0.06	0.58	-0.05
HCO3	0.02	0.01	0	-0.16	0.98	-0.18	-0.2	0.39	0.28	1	0.12	0.02	0.27	0.24
SO4	0.77	0.78	0.15	0.41	0.06	0.6	0.67	0.73	-0.02	0.06	1	0.81	-0.45	0.27
Cl	0.98	0.99	-0.18	0.68	-0.12	0.92	0.97	0.75	0.13	-0.1	0.73	1	-0.32	0.11
NO3	-0.36	-0.34	-0.06	-0.3	-0.17	-0.26	-0.39	-0.31	0.11	-0.19	-0.35	-0.33	1	-0.35
F	0.6	0.57	-0.21	0.43	0.26	0.53	0.61	0.51	-0.12	0.24	0.31	0.54	-0.54	1
Pre-Monsoon														

Factor analyses (PCA) were performed on the hydrogeochemical data set for the pre and post-monsoon periods. The findings of factor analysis are presented in Table 5, which displays the variable loadings, Eigenvalues, and variance accounted for by each factor. In the research region during premonsoon, Factor 1 is characterised by high loadings for EC, TDS, TH, Ca, Na, Mg, Cl, and SO_4, moderate loadings for F, and low loadings for K with a total variance of 48.8%. Factor 2 explains 17.9% of the overall variance; with TA and HCO_3 being heavily and moderately loaded by Na and K. Positive loading of HCO_3 is indicative of the carbonate weathering process. K and NO_3 have significantly loaded in Factor-3, which contributes to roughly 10.2% of the total variation and denotes the use of fertilisers in the agricultural land. Strong loading of pH and moderate loading of SO_4 were observed in the 4^{th} factor. In the case of the post-monsoon season, Factor-1 is significantly represented by EC, TDS, TH, Ca, Mg, SO_4, Cl, and moderately represented by Na, with a total variance of 48.6% indicating the industrial activities. Factor-2 explains 17.4% of the overall variance, with TA, and HCO_3 substantially loaded, Na moderately loaded, and F poorly loaded, indicating the dissolution process of silicates. Factor-3 accounts for 13% of the overall variance and is highly loaded by K and NO_3, which clearly shows biological activity in the soil.

After normalising the data set to Z-scale, the hydrogeochemical parameters of groundwater samples were utilised in the hierarchical cluster analysis (HCA) via Ward's linkage approach. The dendrogram consists of multiple groups, each of which is composed of multiple subgroups and singletons (Figure 5). The groundwater stations are grouped into three major groups during the premonsoon. Cluster 1 of the premonsoon results was comprised of samples 1-3, 6-7, 10, 12-13, 15, 18-20, 22-24, 26-28, and 30-31 with TDS varying between 584 mg/l and 1662 mg/l showing low pollution levels. Cluster 2 with samples 9, 11,

Table 5. Factor analysis (PCA) for the analytical values

Parameters	Pre-Monsoon				Post-Monsoon			
	F-1	F-2	F-3	F-4	F-1	F-2	F-3	F-4
EC	0.99	0.09	-0.06	-0.04	0.98	0.16	-0.05	-0.05
TDS	0.99	0.07	-0.05	-0.03	0.98	0.17	-0.03	-0.07
Ph	-0.12	0.01	-0.03	0.93	-0.05	-0.08	-0.1	-0.85
TH	0.71	-0.16	-0.15	-0.13	0.96	-0.14	-0.05	0.19
TA	-0.07	0.98	-0.01	0.03	0	0.97	0.13	0.06
Ca	0.91	-0.14	-0.04	-0.29	0.89	-0.04	0.06	0.34
Mg	0.95	-0.13	-0.19	-0.15	0.93	-0.21	-0.13	0.06
Na	0.79	0.45	-0.02	0.18	0.7	0.5	-0.06	-0.38
K	0.18	0.37	0.73	-0.04	0.08	0.15	0.82	0.15
HCO3	-0.06	0.98	-0.01	-0.01	0.02	0.97	0.13	0.11
SO4	0.79	0.09	-0.11	0.4	0.86	0.15	-0.31	0.07
Cl	0.99	-0.04	-0.03	-0.07	0.98	0.02	-0.03	-0.08
NO3	-0.32	-0.25	0.7	-0.09	-0.29	0.19	0.84	0
F	0.53	0.33	-0.57	-0.3	0.11	0.33	-0.5	0.46
Total	6.83	2.51	1.43	1.27	6.8	2.4	1.8	1.3
% of Variance	48.8	17.9	10.2	9.1	48.6	17.4	13	9.2
Cumulative %	48.8	66.7	76.9	86	48.6	66	79	88.2

14, 16, 17, 21, and 29 could be classified as contaminated due to their elevated TDS range of 1880 mg/l to 2672 mg/l. Cluster 3 consists of sample 8 with a high TH (4766 mg/l) value, indicating the carbonated nature of the groundwater. Cluster 4 of samples 4, 5, and 25 with higher EC values significantly represents the pollution due to the untreated industrial effluent mixing with the groundwater of the study area. The stations are grouped into four clusters during the post-monsoon. Cluster 1 of samples 1 to 31 (except 5, 11, 14, 19, 21, 25, and 29) is a region with low pollution levels with respect to the lower TDS levels (252 to 1645 mg/l). Cluster 2 consisting of samples 11, 14, and 19, with a mean TDS value of 2352 mg/l, could be classified as moderately polluted. Cluster 3 of samples 5, 21, and 29 with very high EC values of 8450 μS/cm the collection of highly polluted stations. Cluster 4 of sample 25 with an EC value 13280 μS/cm is found to be saline, heavily contaminated and unsuitable for utilisation.

4 Conclusion

Effective use of GIS tools in remote sensing data has been used in this study to explain land use and land cover changes from 1990 to 2021. The interpretation of the results reveals that barren land has changed rapidly during the selected period, decreasing from 7.4 to 4.31 km^2, while built-up land increased dramatically from 21.37 to 24 km^2. Wetland and vegetation land haven't changed much compared to barren and built-up lands. The findings of the LULC change analysis are required to assess the groundwater quality of the Ambattur. Physico-chemical measurements and ionic concentrations indicate that groundwater in numerous areas inside the Ambattur industrial zone is significantly contaminated and unfit for human consumption. The WQI method demonstrates that nearly sixty percent of groundwater is poor to unsuitable during both seasons. Evaporation and rock-water interaction are the primary factors affecting the groundwater chemistry in the studied area. Hydrogeochemical facies diagrams revealed the alternating dominance of alkaline and alkali elements, as well as strong acids and weak acids, as a result of the governing mechanisms. Interpretations of correlation matrices reveal a substantial positive association between all analytical parameters except pH. Analysis of variables and clusters reveals that four key components and a cluster contribute to the interpretation of pollution caused by industrial activity. It is proven with LULC analysis that a constant increase in the built-up land increases the fresh water demand and the existing fresh water is not coping with the population increase. Continuing industrialization and urbanisation will threaten this region's ecosystem. This research can be used to manage urban expansion and plan site-specific industrialization. This study shows that remote sensing and GIS can easily analyse land use and land cover alteration possibilities. It is proposed that adequate artificial recharge structures be constructed at suitable locations to boost the fresh rainwater recharge in order to improve the groundwater quality of the region. Before discharging industrial effluents into open spaces and water storage structures, they should be pre-treated. The local government must implement legislative steps to educate inhabitants of the study area about groundwater contamination in order to protect it for future

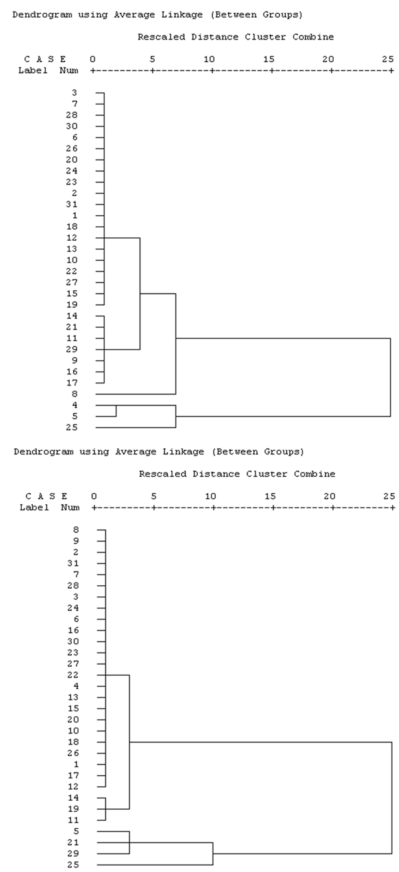

Fig 5. Cluster dendrogram for pre-monsoon and post-monsoon results

development. The comprehensive approach of analysing the LULC changes and the groundwater quality is an added advantage to conclude that anthropogenic activities are deteriorating elements. Since the proposed method in this study requires temporal satellite imagery, the availability of which is questionable. Periodical monitoring of groundwater quality with the LULC change analysis helps to improve the understanding of groundwater systems in such industrial zones. If the same conditions and data are available, this method of analysis can be used in any part of the world. However, periodical collection of both LULC data and hydrogeochemical data will support to build a computational model that can be used predict the future trend of the groundwater quality, especially for the fast-developing metro cities like Chennai. As a result, developing new instrumentation that integrates both the available data for forecasting the changes is the future scope of this present study.

5 Acknowledgment

The authors are thankful to Principal of Presidency College (A), Chennai and HOD of Department of Geography, Presidency College (A), Chennai for providing necessary support to complete the study successfully.

References

1) Sivakumar K, Prabakaran K, Saravanan PK, Muthusamy S, Kongeswaran T, Muruganantham A. Agriculture Drought Management in Ramanathapuram District of Tamil Nadu, India. *Journal of Climate Change*. 2022;8:59–65. Available from: https://doi:10.3233/JCC220005.
2) Thangaraj K, Karthikeyan S. Application of Remote Sensing and GIS in Floodwater Harvesting for Groundwater Development in the Upper Delta of Cauvery River Basin, Southern India. *Water Resources Management and Sustainability*. 2022;p. 257–280. Available from: https://doi.org/10.1007/978-981-16-6573-8_14.
3) Murugesan B, Alemayehu TM, Gopalakrishnan G, Chung SY, Senapathi V, Sekar S, et al. Site selection of check dams using geospatial techniques in Debre Berhan region, Ethiopia — water management perspective. *Environmental Science and Pollution Research*. 2022;29(48):72312–72331. Available from: https://doi.org/10.1007/s11356-021-17232-9.

4) Vellaikannu A, Palaniraj U, Karthikeyan S, Senapathi V, Viswanathan PM, Sekar S. Identification of groundwater potential zones using geospatial approach in Sivagangai district, South India. *Arabian Journal of Geosciences*. 2021;14(8). Available from: https://doi.org/10.1007/s12517-020-06316-4.
5) Sekar S, Kamaraj J, Senapathi V, Sabarathinam C, Viswanathan PM, Karthikeyan S. Delineating saline and fresh water aquifers in Tuticorin of southern India by using geophysical techniques. *Environment, Development and Sustainability*. 2021;23:17723–17744. Available from: https://doi.org/10.1007/s10668-021-01409-w.
6) Muthusamy S, Sivakumar K, Shanmugasundharam A, Jayaprakash M. Appraisal on water chemistry of Manakudy estuary. *India Shengtai Xuebao/ Acta Ecol Sin*. 2021;41(5):463–78. Available from: https://doi.org/10.1016/j.chnaes.2021.07.004.
7) Arumugam M, Karthikeyan S, Thangaraj K, Kulandaisamy P, Sundaram BP, Ramasamy K, et al. Hydrogeochemical Analysis for Groundwater Suitability Appraisal in Sivagangai, an Economically Backward District of Tamil Nadu. *Journal of the Geological Society of India*. 2021;97(7):789–798. Available from: https://doi.org/10.1007/s12594-021-1761-8.
8) Ramachandran A, Sivakumar K, Shanmugasundharam A, Sangunathan U, Krishnamurthy RR. Evaluation of potable groundwater zones identification based on WQI and GIS techniques in Adyar River basin, Chennai, Tamilnadu, India. *Acta Ecologica Sinica*. 2021;41(4):285–295. Available from: https://doi.org/10.1016/j.chnaes.2020.02.006.
9) Kulandaisamy P, Karthikeyan S, Chockalingam A. Use of GIS-AHP tools for potable groundwater potential zone investigations—a case study in Vairavanpatti rural area, Tamil Nadu, India. *Arabian Journal of Geosciences*. 2020;13:866. Available from: https://doi.org/10.1007/s12517-020-05794-w.
10) Karthikeyan S, Kulandaisamy P, Senapathi V, Chung SY, Thangaraj K, Arumugam M, et al. Hydrogeochemical Survey along the Northern Coastal Region of Ramanathapuram District, Tamilnadu, India. *Applied Sciences*. 2022;12(11):5595. Available from: https://doi.org/10.3390/app12115595.
11) Karthikeyan S, Arumugam S, Muthumanickam J, Kulandaisamy P, Subramanian M, Annadurai R, et al. Causes of heavy metal contamination in groundwater of Tuticorin industrial block, Tamil Nadu, India. *Environmental Science and Pollution Research*. 2021;28:18651–18666. Available from: https://doi.org/10.1007/s11356-020-11704-0.
12) Ram A, Tiwari SK, Pandey HK, Chaurasia AK, Singh S, Singh YV. Groundwater quality assessment using water quality index (WQI) under GIS framework. *Applied Water Science*. 2021;11:46. Available from: https://doi.org/10.1007/s13201-021-01376-7.
13) Chaudhry AK, Sachdeva P. GIS-based groundwater quality assessment using GQIs and fuzzy-logic approach. *Water and Environment Journal*. 2022;36:172–182. Available from: https://doi.org/10.1111/wej.12738.
14) Kumar S, Elango PJ, Schneider L, M. GIS and AHP Based Groundwater Potential Zones Delineation in Chennai River Basin (CRB), India. *Sustainability* . 2022;14(3):1830. Available from: https://doi.org/10.3390/su14031830.
15) Castillo JLU, Cruz DAM, Leal JAR, Vargas JT, Tapia SAR, Celestino AEM. Delineation of Groundwater Potential Zones (GWPZs) in a Semi-Arid Basin through Remote Sensing, GIS, and AHP Approaches. *Water*. 2022;14(13):2138. Available from: https://doi.org/10.3390/w14132138.
16) Singh B, Venkatramanan V, Deshmukh B. Monitoring of land use land cover dynamics and prediction of urban growth using Land Change Modeler in Delhi and its environs, India. *Environmental Science and Pollution Research*. 2022;29:71534–71554. Available from: https://doi.org/10.1007/s11356-022-20900-z.
17) Derdour A, Benkaddour Y, Bendahou B. Application of remote sensing and GIS to assess groundwater potential in the transboundary watershed of the Chott-El-Gharbi (Algerian–Moroccan border). *Applied Water Science*. 2022;12:136. Available from: https://doi.org/10.1007/s13201-022-01663-x.
18) Standard Methods for the Examination of Water and Wastewater. *APHA*. 2017.
19) Mondal BK, Sahoo S, Das R, Mishra PK, Abdelrahman K, Acharya A, et al. Assessing Groundwater Dynamics and Potentiality in the Lower Ganga Plain, India. *Water*. 2022;14(14):2180. Available from: https://doi.org/10.3390/w14142180.
20) Ramasamy V, Alotaibi Y, Khalaf OI, Samui P, Jayabalan J. Prediction of groundwater table for Chennai Region using soft computing techniques. *Arabian Journal of Geosciences*. 2022;15:827. Available from: https://doi.org/10.1007/s12517-022-09851-4.
21) Vignesh KS, Thambidurai P, Selvan VNI, Adhikary PP, Shit PK, Santra P, et al. Geostatistics and Geospatial Technologies for Groundwater Resources in India. S B, editor;Tamil Nadu, India; Cham. Springer Hydrogeology. Springer. 2021. Available from: https://doi.org/10.1007/978-3-030-62397-5_9.
22) Al-Tameemi IM, Hasan MB, Al-Mussawy HA, Al-Madhhachi AT. Groundwater Quality Assessment Using Water Quality Index Technique: A Case Study of Kirkuk Governorate, Iraq. *IOP Conference Series: Materials Science and Engineering*. 2020;881:012185. Available from: https://doi:10.1088/1757-899X/881/1/012185.
23) Guidelines for drinking-water quality, world health organization. *WHO*. 2016;1:631.
24) Gibbs R. Mechanisms Controlling World Water Chemistry. *Science*. 1970;170(3962):1088–1090. Available from: https://doi:10.1126/science.170.3962.1088.
25) A graphic procedure in the geochemical interpretation of water analysis. *Trans Am Geophys Union*. 1944;25:914–923. Available from: https://doi.org/10.1029/TR025i006p00914.